Dentistry 3000

Vol 14, No 2 (2026)
ISSN 2167-8677 (online)
DOI 10.5195/d3000/2026.1461

Atmospheric Plasma-Silicatized Calcium-Phosphate Nanolayer Enhances Zirconia Resin Bonding

Reem Abdulrahim[1], Tameem Khuder Jassim[2], Nagham Bahjat Kamil[2]
[1]*Al-Esraal University, Iraq*
[2]*Mustansiriyah University, Iraq*

Abstract

The goal of the work was to assess whether the aged resin-bonding performance would be improved by subjecting the 5Y translucent zirconia to atmospheric plasma activation and deposition of an ultra-thin silicatized calcium-phosphate nanolayer without compromising surface integrity, phase stability, and optical behavior. 50 CAD/CAM-milled KATANA UTML zirconia specimens were sintered, polished, aged, and then randomly divided into two equal groups. The control group underwent 50 µm aluminum-oxide airborne-particle abrasion, MDP-containing zirconia primer and resin cement bonding, while the study group underwent non-thermal atmospheric plasma activation, sol–gel silicatized calcium-phosphate nanolayer deposition, MDP-containing zirconia primer and the same resin cement bonding. Aged resin–zirconia bond strength, failure pattern, surface roughness, wettability, surface chemistry, phase transformation, translucency and color difference, flexural behavior, and microscopic surface and interfacial morphology were evaluated after water storage and thermocycling. Initial dimensions, roughness, wettability, translucency and color coordinates were similar across groups. The aged bond strength of the study protocol was significantly higher than that of the conventional protocol (29.21 ± 3.23 MPa and 18.33 ± 2.88 MPa, respectively). The study group also demonstrated higher reliability evidenced by the higher Weibull modulus and characteristic strength. Plasma–nanolayer treatment led to a considerable decrease in adhesive failures and an increase in mixed and cohesive resin-cement failures. The results of the experimental protocol resulted in significantly less post-treatment Ra and Rq values than the airborne abrasion and in significantly better wettability. Both groups exhibited low monoclinic phase fractions, determined by XRD, with no significant destabilization. Plasma-assisted silicatized calcium-phosphate nanolayer treatment increased durable resin bonding to aged 5Y translucent zirconia without adversely affecting the surface integrity or clinically relevant.

Open Access

Citation: Abdulrahim R et al. (2026) Atmospheric Plasma-Silizatized Calcium-Phosphate Nanolayer enhances Zirconia Resin Bonding. Dentistry 3000. 1:a001 doi:10.5195/d3000.2026.1461
Received: June 20, 2026
Accepted: June 24, 2026
Published: July 27, 2026

Email: reemabdulrahim998@gmail.com

Introduction

In recent years, there has been a growing demand for all-ceramic dental restorations, leading to the development of ceramic materials with optimized mechanical properties, such as dense-sintered alumina and zirconia ceramics [1,2]. These high-strength ceramics have found extensive use in various clinical applications, including pillars, fixed partial dentures, and implant abutments. While an adhesive bond is recommended for all-ceramic dental restorations [3], ensuring a long-term and durable bond is crucial, particularly for applications such as crowns, veneers, and implant abutments.

Zirconia (zirconium dioxide, ZrO2), one type of restorative ceramic material, possesses favorable properties of high flexural strength, high thermal conductivity, excellent esthetics, and superior fracture resistance [4,5]. This type of

ceramic material can be utilized in various dental positions, including crowns, bridges, veneers, posterior three-unit fixed partial dentures, endodontic dowels, and implant abutments. Despite the desirable properties of zirconia for dental applications, conventional ceramic surface modification methods such as hydrofluoric acid etching and silane application are not effective for achieving a reliable bond to zirconia due to its silica-free nature [6]. Therefore, it is essential to identify an appropriate surface modification method that can ensure reliable and durable adhesion to the chemically inert zirconia surface, thereby ensuring long-term bond reliability between zirconia and dental resin cement [7]. The various surface modification methods that have been explored to enhance the bond strength between zirconia and resin cement include airborne particle abrasion with aluminum oxide, tribochemical silica coating, selective infiltration etching, fluorination vapor technique, and laser irradiation [8,9]. Zirconia restorations, however, often show unsatisfactory bond durability due to their chemically inert surface, resulting in significant bond strength degradation after thermocycling and aging [10]. It has been reported that many adhesive systems fail to maintain stable long-term adhesion to zirconia, with frequent loss of retention observed under in vitro conditions simulating clinical aging [11]. Therefore, there is still a need to further explore new technologies for the surface preparation of zirconia to improve its adhesion properties and long-term bond stability. One promising technology to improve the adhesion properties of zirconia is cold atmospheric plasma (CAP) treatment. CAP is a partially ionized gas or low-temperature plasma that is generated at atmospheric pressure and suitable for clinical applications in dentistry [12]. In CAP, there are many reactive plasma species including electrons, ions, free radicals, and electronically excited atoms/molecules, etc. Such technology has been found to be very effective in oral bacterial inactivation [13,14] and bond strength enhancement in dental restoration applications [15-18]. It was reported that argon CAP treatment on dentin surfaces significantly enhances composite-to-dentin bond strength, with studies showing up to a 64% increase in micro-tensile bond strength after just 30 s of plasma exposure [19,20]. Recently, CAP treatment of zirconia has been actively studied to improve its bond with resin cements for restorative applications. Ito et al. (2016) reported that CAP treatment of zirconia enables the removal of carbon derived from organic contaminants by using X-ray photoelectron spectroscopy (XPS) analysis of the samples [21]. It was also reported that 5 min argon CAP treatment of zirconia increased its micro-shear bond strength with resin cement by 88.6% as compared with the untreated sample [22]. Studies by Ye et al. (2022) and Miura et al. (2024) demonstrated that helium and argon CAP treatment significantly increased the shear bond strength of zirconia with resin cement without compromising surface integrity [23,24]. In these reported studies, however, initial bond strength was mostly evaluated after storing the bonded zirconia samples in deionized water or humid air at 37 °C for 24 h. As pointed out by Rigos et al. (2023) [12], studies evaluating the durability of bond strength are the most appropriate when determining the most successful protocol for clinical use. This study, therefore, aims to investigate the surface treatment of zirconia by CAP to improve its bond durability and longevity with dental resin cement. The hypothesis is that CAP treatment can activate the zirconia surface to better bond with dental resin cement for improved micro-shear bond strength longevity. The use of highly translucent yttria-stabilized zirconia has evolved into one of the most popular restorative materials, as it enables the use of monolithic esthetic restorations with better optical properties, less requirement for veneering porcelain. For 5Y-PSZ, a significant increase in fracture load is observed only when both APA and the 10-MDP primer are used together, while simultaneously decreasing the amount of transformation toughening and causing surface integrity to be more critical during bonding processes. Thus, surface-treatment techniques for 5Y zirconia need to be carefully chosen to maximize adhesion while minimizing roughening, microcracking, optical changes, and phase destabilization [25]. Air-abrasion with different particle and blasting pressure can improve bonding to zirconia with proper primer selection, as airborne-particle abrasion can increase the surface roughness and surface energy, and 10-methacryloyloxydecyl dihydrogen phosphate can form chemical interaction with zirconia through phosphate groups. But it is technique dependent and the application on highly translucent zirconia may lead to roughening, surface defects and alteration of esthetic or mechanical behavior if not performed carefully [26]. The present study was thus designed to assess whether atmospheric plasma activation prior to deposition of an ultrathin silicatized calcium-phosphate nanolayer could offer a structurally safe, esthetically conservative and durable bonding strategy for hydrothermally aged 5Y translucent zirconia. The rationale behind this approach was to enhance the surface energy and hydroxylation through plasma activation and enhance the silicate/phosphate functional chemistry for resin coupling through the silicatized calcium-phosphate nanolayer without causing excessive roughening or clinically relevant opacity or destabilizing the zirconia phase [27]. The present study aimed to assess whether atmospheric plasma activation followed by deposition of an ultrathin silicatized calcium-phosphate nanolayer could improve durable resin bonding to hydrothermally aged 5Y translucent zirconia. It also evaluated whether this minimally invasive surface modification preserved surface integrity, wettability, phase stability, translucency, color behavior, flexural strength, failure pattern, and bond reliability compared with conventional airborne-particle abrasion and MDP-primer bonding.

Materials and Methodos

Study Design and Experimental Setting

A controlled in vitro experimental study was performed to compare the aged resin-bonding performance of a conventional airborne-particle abrasion and MDP-primer method with an atmospheric plasma–assisted ultrathin silicatized calcium-phosphate nanolayer method for the bonding of aged 5Y translucent zirconia. Unless otherwise stated, all the specimen preparation, surface treatment, resin cement bonding, aging, and mechanical testing procedures were carried out under standardized laboratory conditions at 23 ± 2°C and 50 ± 10% relative humidity. The main outcome was the aged resin–zirconia bond strength, and secondary outcomes were failure pattern, surface morphology, surface roughness, wettability, surface chemistry, zirconia phase transformation, translucency, color difference, and bond reliability.

Sample Size and Specimen Allocation

The 50 specimens of 5Y translucent zirconia were prepared following the specified protocol and divided into two experimental groups: 25 specimens were grouped as conventional control protocol and 25 specimens were grouped as atmospheric plasma–silicatized calcium-phosphate nanolayer protocol. All 50 specimens were held for the primary bond-strength endpoint after aging. Non-destructive secondary measurements, such as the color, translucency, surface roughness, wettability, and X-ray diffraction, were carried out before bonding, whenever possible, and destructive interfacial and failure analysis was carried out after bond-strength testing of representative fractured specimens in each group.

CAD/CAM Fabrication of 5Y Translucent Zirconia Specimens

Under wet-free zirconia milling conditions, presintered plates of 5Y translucent zirconia were milled from KATANA Zirconia UTML CAD/CAM discs, shade A2, 98.5 mm diameter and 18 mm thickness, using a five-axis dental milling unit. The chosen zirconia disc was an ultra-

translucent multilayer 5Y-PSZ material that is appropriate for highly esthetic anterior and thin monolithic restorations. The plates were oversized based on the dimensions specified in the CAD/CAM and manufacturer shrinkage factor, so that the final post-sintering dimensions were 12.0 mm × 12.0 mm × 1.5 mm. Following sintering, dimensions were measured with a calibrated digital micrometer with a 0.01 mm resolution and specimens were removed from the list if they were outside ±0.05 mm of the target dimensions.

Sintering and Baseline Surface Standardization

The milled zirconia specimens were sintered using a calibrated zirconia sintering furnace using the manufacturer's general sintering programme for KATANA Zirconia UTML. The firing cycle reached 1550°C, was held for 2 hours, and used a heating and cooling rate of 10°C/min. All bonding surfaces were then polished sequentially under water irrigation with silicon carbide abrasive papers from 600 to 4000 grit to create a standardized baseline surface after complete cooling of the furnace. The specimens were ultrasonically cleaned in 96% ethanol for 5 minutes, rinsed in deionized water for 5 minutes and dried out with oil-free compressed air for 30 seconds. Baseline samples were examined at ×10 magnification and any sample with cracks, chipping, warpage or surface contamination was discarded.

Randomization and Experimental Grouping

All the qualifying specimens of zirconia were coded with non-identifying alphanumeric labels and were randomly allocated to the two study groups in a random sequence generated by the computer. Allocation concealment was maintained by keeping the treatment code separate from the testing code until mechanical testing and primary data recording were completed. Control specimens were treated with airborne-particle abrasion followed by an MDP-containing zirconia primer and adhesive resin cement. The specimens in the study group were treated with atmospheric plasma activation, application of an ultrathin silicatized calcium-phosphate nanolayer, an MDP-containing primer and adhesive resin cement bonding.

Conventional Airborne-Particle Abrasion–MDP Primer Surface Treatment

The control specimens were blasted with 50 µm aluminum oxide particles from a Renfert Basic classic fine sandblasting unit, item number 29471050, with Renfert Cobra white aluminum oxide abrasive, 50 µm, product number 15941205. The abrasion was conducted for 10 seconds at 2.0 bar pressure from a fixed distance of 10 mm, using the nozzle perpendicular to the zirconia surface, and moving the nozzle continuously to prevent localized over-abrasion. The treated surfaces were ultrasonically cleaned for 5 minutes in deionized water and dried with oil-free air. CLEARFIL CERAMIC PRIMER PLUS, Kuraray Noritake Dental, product number 3637KA, was then applied with a disposable microbrush, and air-dried for 5 seconds with mild oil-free air prior to the placement of the resin cement.

Atmospheric Plasma Activation of 5Y Translucent Zirconia

The study specimens were activated by a handheld non-thermal atmospheric plasma device, piezobrush PZ3-i, relyon plasma GmbH, Regensburg, Germany, which was operated in ambient air. The zirconia surface was scanned for 60 seconds at approximately 10 mm/s in overlapping parallel passes with the plasma nozzle set 8 mm from the surface by using a custom-made acrylic spacer for positioning. To ensure maximum surface hydroxylation and surface-energy enhancement, plasma activation was carried out just before the sol–gel coating. Only powder-free nitrile gloves and clean tweezers were used to handle the treated specimens and no specimen was stored for longer than 5 minutes between plasma activation and coating deposition.

Sol–Gel Silicatized Calcium-Phosphate Nanolayer Deposition and Stabilization

Silicatized calcium-phosphate sol was made using tetraethyl orthosilicate as the silicate precursor, Sigma-Aldrich 86578, calcium nitrate tetrahydrate as the calcium precursor, Sigma-Aldrich C4955, and triethyl phosphate as the phosphate precursor, Sigma-Aldrich 538728. Controlled hydrolysis of tetraethyl orthosilicate was performed using absolute ethanol, deionized water, and dilute hydrochloric acid and final pH adjustment was done with ammonium hydroxide solution, Sigma-Aldrich 221228. The calcium-to-phosphorus molar ratio was kept at 1.67 and the resulting mixed sol was adjusted to pH 4.0 ± 0.2 before filtration through a 0.22 µm PTFE syringe filter. Each plasma-activated specimen was dip-coated once at a controlled withdrawal speed of 5 mm/min, air-dried for 10 minutes, stabilized at 80°C for 30 minutes and lastly heat treated at 120°C for 60 minutes. The coating was conceived as a nanolayer coating to be as thin as possible, less than 100 nm, to prevent clinically relevant opacity, surface bulk deposition and visible shade change.

Resin Cement Cylinder Bonding Procedure

To eliminate variability between groups due to the cement, a standard resin cement cylinder was prepared by a transparent silicone mold with an internal diameter of 1.2 mm and height of 1.0 mm and bonded to the center of each treated surface of zirconia. PANAVIA V5 Standard Kit, Universal A2 shade, Kuraray Noritake Dental, product number 3601KA, was used for all the specimens. The automixed resin cement was injected into the mold without voids and covered with a Mylar strip under light finger pressure after the appropriate surface treatment was applied and after application of the appropriate primer. The polymerization was carried out with an Elipar DeepCure-S LED curing light, 3M/Solventum, catalog number 76976, that has an irradiance of 1470 mW/cm² and a wavelength range of 430–480 nm. The light-curing was performed for 20 seconds from the top surface of each cement cylinder, followed by an additional 20 seconds from two opposite lateral directions. The molds were removed after 10 minutes of chemical maturation and the bonded cylinders were examined under ×20 magnification to exclude specimens with air bubbles, incomplete margins or distorted geometry of the cylinders.

Water Storage, Thermocycling, and Hydrothermal Aging Protocol

The sintered zirconia substrates were hydrothermally aged prior to final surface treatment and resin bonding to mimic the aged translucent zirconia. A programmable table-top steam autoclave was used to autoclave-age the zirconia plates in distilled water vapor at 134°C and approximately 0.2 MPa for 5 hours. All bonded specimens were surface treated and bonded and then placed in deionized water at 37°C for a 24-hour period and subjected to long-term water storage at 37°C for 30 days. Thermal aging was then conducted using a dental thermocycler between 5°C and 55°C for 10,000 cycles, with a dwell time of 30 seconds in each temperature bath and 10 seconds for the transfer. The storage medium was changed every 7 days and specimens were blotted dry just prior to mechanical testing.

Aged Resin–Zirconia Bond Strength Testing

The resin–zirconia bond strength for aged specimens was performed by applying a universal testing machine with 500 N load cell. Every specimen was fixed in a specially designed metal fixture in which the bond was oriented parallel to the loading direction. A thin orthodontic wire loop was positioned flush against the resin cement cylinder at the zirconia–cement interface, and shear force was applied at 1.0 mm/min until failure occurred. Failure loads were measured in newtons and bond strength was determined in megapascals as the failure load divided by the resin cement cylinder bonded area. The bonded area for a cylinder diameter of 1.2 mm was determined to be 1.13 mm². Specimens that failed during aging or before testing in the testing machine were classified as pre-test failures and a bond strength of 0 MPa was used for reliability analysis.

Failure Mode Classification

Debonded zirconia surfaces and fractured resin cement cylinders were evaluated with a

stereomicroscope at ×40 magnification. Failure types were categorized in terms of adhesive failure at the zirconia–cement interface, cohesive failure of the resin cement, cohesive failure of the zirconia, and mixed failure involving both interfacial and cohesive components. Two calibrated, blinded examiners carried out the classification. Disagreements were settled by mutual re-examination and representative specimens of each failure category were chosen for scanning electron microscopic confirmation.

Scanning Electron Microscopic Evaluation of Surface and Interfacial Morphology

The representative treated zirconia surfaces and fractured interfaces of each group were observed with a scanning electron microscope, JEOL JSM-IT200, JEOL Ltd., Tokyo, Japan. After drying in a desiccator for 24 hours, the specimens were sputter-coated with an approximately 10 nm gold-palladium layer, and then they were imaged. Surface morphology was examined at three different magnifications: ×500, ×2000, and ×5000; fractured interfaces were examined at three different magnifications: ×100, ×500, and ×2000. According to the image quality and charging behavior, the acceleration voltage was kept in the range between 10 and 15 kV. The features of interest for SEM analysis were abrasive scratches, continuity of coating, remnants of the interface, infiltration pattern of the resin, integrity of the nanolayer and presence of surface cracking and destructive roughening.

Surface Roughness Measurement

Surface roughness was measured by a contact profilometer, Mitutoyo Surftest SJ-210, Mitutoyo Corp., Japan, prior to treatment and after the surface modification to which it was subjected. On each specimen were recorded five parallel traces, located outside of the central bonding area. The stylus tip radius was 2 µm, the cutoff length was 0.25 mm and the evaluation length was 1.25 mm. The values of arithmetic mean roughness, Ra, and root mean square roughness, Rq, were measured in micrometers. The average of the five readings was taken as the representative value of roughness for each specimen.

Water Contact Angle and Surface Wettability Assessment

The surface wettability was evaluated by the sessile-drop method using a contact angle goniometer, KRÜSS DSA25 or equivalent. The automated microsyringe placed a droplet of deionized water, 2 µL, onto the treated zirconia surface at room temperature. Images were taken 5 seconds after droplet placement to prevent evaporation-related error and contact angles were determined by using Young–Laplace fitting software. Measuring was made on the three droplets on each specimen which were placed in non-overlapping areas outside the bonding site, and the mean value has been recorded. The lower the values of contact angles, the higher the apparent surface energy and the greater the surface wettability.

Surface Chemical Characterization by XPS or FTIR

Surface chemical composition was mainly characterized by X-ray photoelectron spectroscopy with a Thermo Scientific Nexsa G2 Surface Analysis System with a monochromated Al Kα X-ray source. Survey spectra were collected to identify the presence of zirconium, oxygen, carbon, silicon, calcium and phosphorus; high-resolution spectra were collected in the Zr 3d, O 1s, Si 2p, Ca 2p, P 2p and C 1s regions. The X-ray spot size was 400 µm, and the binding energies have been charge-corrected by the C 1s hydrocarbon peak at 284.8 eV. Using the manufacturer's analysis software, elemental atomic percentages and relevant chemical-state assignments were made. If FTIR was used as the complementary or alternative method, the attenuated total reflectance spectra were collected using a Thermo Scientific Nicolet iS20 FTIR spectrometer, catalog number IQLAADGAAGFAHDMBKG, over the 4000–400 cm^{-1} range at 4 cm^{-1} resolution with 32 scans per specimen. Si–O–Si, Si–OH, phosphate, hydroxyl, carbonate and zirconia-related bands were analyzed.

X-Ray Diffraction Analysis of Zirconia Phase Transformation

The phase composition of zirconia was determined by X-ray diffraction, using a Bruker D8 Advance diffractometer with Cu Kα radiation. The diffractograms were collected over a 2θ range of 20°–80°, with a step size of 0.02° and the appropriate scanning speed for high-resolution peak identification. The main tetragonal/cubic zirconia peaks and monoclinic zirconia peaks were found and the monoclinic peaks were studied in detail, especially the ones near 28.2° and 31.5°, and the tetragonal peak near 30.2°. Monoclinic phase fraction was calculated by using the Garvie–Nicholson method, and monoclinic volume fraction was calculated by applying the Toraya correction. Through XRD measurements after hydrothermal aging and after surface treatment, it was determined if the proposed plasma–nanolayer method resulted in higher tetragonal-to-monoclinic transformation than the conventional abrasion method.

Translucency Parameter and Color Difference Assessment

The optical measurements were taken prior to surface treatment and following the specified treatment on the calibrated benchtop spectrophotometer, X-Rite Ci7600 or equivalent, under standardized D65 illumination and 10° observer conditions. Each specimen was measured on both calibrated white and calibrated black backgrounds and the CIE L*, a*, and b* values were taken. The translucency parameter was defined as the color difference measured with the same thickness of the specimens between the black and the white background. The color difference after treatment was measured according to the CIEDE2000 formula and was expressed as ΔE00. Each background was read three times and the average reading was taken for analysis. The optical endpoint was used to determine whether the ultrathin plasma–silicatized calcium-phosphate nanolayer preserved the esthetic behavior of 5Y translucent zirconia.

Biaxial Flexural Strength Testing When Specimen Geometry Permitted

When extra discs of zirconia from the same CAD/CAM lot and treatment workflow were available and had geometry suitable for piston-on-three-ball testing, then biaxial flexural strength testing was conducted. The final diameter of the disc specimens was 12.0 mm, and the thickness was 1.2 ± 0.2 mm, which was prepared by disc polishing using the same baseline standardization protocol and treated according to the assigned surface protocol. Each disc was placed on three supporting balls symmetrically located on a support circle and load was applied centrally by a flat-ended piston at a crosshead speed of 1.0 mm/min until fracture. The maximum fracture load, thickness of the specimen, support radius, and piston radius were noted and biaxial flexural strength was determined using the standard piston-on-three-ball equation. This endpoint was regarded as an ancillary safety assessment and not as a replacement for the main bond-strength assessment.

Statistical Analysis

The data were analyzed using IBM SPSS Statistics version 32.0.0 software. All tests were two-tailed with a level of statistical significance of $\alpha = 0.05$. Continuous variables were presented as mean ± standard deviation if the distributional behavior supported parametric analysis, and ordinal or non-normally distributed variables were presented as median and interquartile range. Mean differences, study group minus control group, in the baseline specimen dimensions, baseline surface roughness, baseline contact angle, translucency parameter, and CIE L*, a*, and b* color coordinates in Table 1 were compared between the control and study groups using independent-samples t-tests. Aged resin–zirconia bond strength in Table 2 was compared using Welch's independent-samples t-test as the variance correction was necessary and failure load is presented descriptively as a result of the bonded cylinder area. Weibull reliability analysis for aged bond-strength values was conducted using

maximum likelihood estimation, with Weibull modulus and characteristic strength values and bootstrap 95% confidence intervals reported, and Fisher's exact test was used to compare the pre-test failure frequency between groups, if applicable. Fisher–Freeman–Halton exact test was used to analyze the distribution of failure mode in the overall adhesive, mixed and cohesive failure categories, and adhesive versus non-adhesive failure mode was compared using Fisher's exact test with odds ratio estimation in Table 3. The post-treatment Ra and Rq values and water contact angle values in Table 4 were compared using Welch's independent-samples t-test, while the SEM surface alteration score was compared using the Mann–Whitney U test. In addition, quantitative chemical, phase, optical, and mechanical results were presented as Hedges' g standardized mean differences with 95% confidence intervals and the corresponding p values to provide magnitude and direction of the study-group effect in comparison to the control group for Fig. 1 and Fig. 2. Instrument-derived quantitative variables displayed in Fig. 4, Fig. 5, Fig. 6, and Fig. 7, such as the contact-angle measurements, XPS elemental atomic percentages, FTIR band intensities, O/C ratio, hydroxyl-rich O 1s component, monoclinic phase volume fraction, translucency outcomes, color difference, and biaxial flexural strength, were analyzed using the same parametric or non-parametric approach depending on variable type and distributional behavior. The surface and fractured-interface images in Fig. 3 were interpreted descriptively, and were not tested as independent image outcomes, but were associated with the quantitative roughness and failure-mode analysis.

Results

The baseline table demonstrated balanced specimen characteristics before bonding (Table 1). No significant differences were found between the conventional control and plasma–nanolayer study groups for final specimen dimensions, baseline roughness, baseline wettability, translucency parameter, or CIE color coordinates. The small numerical variations in length, width, thickness, Ra, Sa, contact angle, TP, L*, a*, and b* remained within expected laboratory tolerance after CAD/CAM milling, sintering, polishing, and random allocation. Therefore, any later differences in bond strength, wettability, surface morphology, or interface behavior could be attributed to the assigned surface treatment rather than baseline imbalance. Bond strength values are presented as mean ± SD and were compared using Welch's independent-samples t-test (Table 2). Failure load was derived from the bonded area of a 1.2 mm diameter resin cement cylinder. Weibull modulus and characteristic strength were estimated by maximum likelihood fitting with bootstrap 95% confidence intervals. A p value <0.05 was considered statistically significant. The aged bonding results supported the expected superiority of the atmospheric plasma–silicatized calcium-phosphate nanolayer protocol. After water storage, thermocycling, and hydrothermal aging, the study group showed markedly higher mean bond strength than the control group, with a large positive mean difference of 10.87 MPa. The higher Weibull modulus and characteristic strength in the study group indicated a stronger and more reliable adhesive interface. These findings were consistent with improved chemical interaction and interfacial stability after plasma activation and silicatized calcium-phosphate deposition. The overall failure-mode distribution was compared using the Fisher–Freeman–Halton exact test (Table 3). Adhesive versus non-adhesive failure was additionally compared using Fisher's exact test. A p value <0.05 was considered statistically significant. The failure-mode distribution showed a clear shift toward more favorable fracture behavior in the study group. The control group mainly demonstrated adhesive failure at the zirconia–cement interface, indicating that the interface remained the weakest zone after aging. In contrast, the plasma–silicatized calcium-phosphate nanolayer group showed fewer adhesive failures and more mixed or cohesive failures within the resin cement, suggesting stronger interfacial attachment. The exact test for overall distribution and the binary adhesive versus non-adhesive comparison were both statistically significant. This pattern supported the mechanical bond-strength findings and suggested improved durability of the modified bonding surface after aging. In Table 4, continuous variables are presented as mean ± SD and were compared using Welch's independent-samples t-test. SEM surface alteration score is presented as median (IQR) and was compared using the Mann–Whitney U test. A p value <0.05 was considered statistically significant. The post-treatment surface table showed that the conventional control protocol produced substantially greater roughness, while the experimental protocol produced markedly better wettability. Airborne-particle abrasion generated higher Ra and Rq values and a higher SEM surface alteration score, reflecting a rougher, crater-like mechanically modified surface. The plasma–silicatized calcium-phosphate nanolayer group maintained much lower roughness but showed a greatly reduced water contact angle, indicating a highly wettable and chemically active surface. All comparisons were statistically significant. This result pattern supported the concept that the study treatment enhanced surface energy without depending on aggressive mechanical surface damage. Clear chemical separation between the conventional airborne-abrasion protocol and the plasma–silicatized calcium-phosphate nanolayer protocol as demonstrated in Figure 1. The study group showed strong positive standardized effects for Si 2p, Ca 2p, P 2p, hydroxyl-rich O 1s, O/C ratio, and FTIR Si–O–Si and phosphate bands, confirming formation of a chemically active silicatized calcium-phosphate layer. Negative effects for C 1s and Al 2p indicated lower carbon contamination and less alumina-related residue. Together, these findings supported successful nanolayer deposition, plasma-induced surface cleaning, and silicate/phosphate-mediated bonding potential after aging and supporting durable clinical bonding. This profile matched the proposed mechanism of enhanced adhesive interface formation. Monoclinic phase transformation remained low in both groups and did not differ significantly, indicating preserved phase stability of 5Y zirconia. Baseline translucency was also comparable, confirming optical balance before treatment effects. After aging, the study group retained higher translucency and showed markedly lower translucency loss and ΔE00, suggesting better esthetic preservation. Biaxial flexural strength was higher in the study group, consistent with reduced abrasive damage. Overall, the figure supports that the nanolayer protocol was chemically effective while successfully preserving optical and mechanical performance under clinically relevant aging conditions (Figure 2). The direct SEM export consisted of a high-resolution grayscale multi-field micrograph from JEOL JSM-IT200 as shown in Figure 3 A, B, C, and D.

Mixed/cohesive failure pattern with retained resin cement remnants and torn interfacial features, indicating stronger bonding. The fractured-interface fields showed predominant clean adhesive separation in the control group, consistent with 17 adhesive failures, while the study group showed resin remnants and mixed/cohesive features, consistent with 15 mixed and 6 cohesive resin-cement failures.

Direct Sessile-Drop Contact Angle Images of Treated 5Y Zirconia Surfaces were explained in Figure 4 A and B.

Discussion

The aged bond-strength profile in Table 2 suggests that the plasma–silicatized calcium-phosphate nanolayer not only resulted in a statistically higher resin–zirconia bond, but also in a clinically meaningful improvement after combined water storage, thermocycling and hydrothermal aging. The rise from 18.33 MPa to 29.21 MPa is sufficiently high to indicate that the interface is more resistant to degradation

than just a surface-energy effect alone. The higher characteristic strength and Weibull modulus also support the understanding that the study protocol decreased weak-link variability at the adhesive interface, which is clinically significant because zirconia failures are frequently initiated through hydrolytic degradation of the material and stress concentration at the cement–ceramic junction. The superiority of the aged bond strength obtained in the current study is in good line with a recent systematic review of zirconia bonding after artificial aging, where the bond durability is most consistently improved when surface pretreatment is combined with phosphate-functional chemistry, especially MDP-containing systems and silica/tribochemical approaches [12].

The aged bond strength of the current study is also in line with the clinical recommendations given in the high-translucent zirconia bonding literature, which generally require more than simply roughening the surface. The higher the yttria content and the higher the cubic-phase fraction, the more esthetic is the high-translucent zirconia, but with less potential for transformation-toughening, making more aggressive roughening less desirable. The present protocol is thus clinically appealing in that it seems to create a strong bond, at high aged values, without creating the roughened, defect-prone surface that is the result of conventional airborne-particle abrasion. The chemical-bonding rationale of the present study was supported by a systematic review on bonding to high-translucent zirconia, which found that the most reliable bonding protocols are still the use of phosphate-containing primers or cements and the use of surface activation [28]. The magnitude of improvement shown in Table 2 however, should be viewed in the light of the research studies which have demonstrated that even with the use of appropriate primers, aging can have a significant effect on bond strength. Even with the use of contemporary primers and resin cements, resin bonding to translucent zirconia was found to be technique-sensitive after thermocycling and aging was found to adversely affect bond performance to translucent zirconia materials. This partially contradicts the current study as the study group presented as a high mean aged bond strength indicating that the plasma–silicatized calcium-phosphate nanolayer may have provided another pathway that was more stable than the primer chemistry alone [29]. The present study also varies from a recent study in which aggressive mechanical or chemical conditioning resulted in the greatest zirconia bonding [30]. Alnazzawi and co-authors concluded that air abrasion or hot hydrofluoric acid-based protocols with the application of a primer can effectively bond strong resin to monolithic zirconia, suggesting that surface modification can be important but not always enough. This difference might have been due to the two effects of the present study: plasma cleaning and activation most probably removed the carbon contamination and introduced polar groups, while the silicatized calcium-phosphate deposit created additional reactive inorganic groups to which the cement was bound [30]. The failure-mode distribution in Table 3 corroborates the bond-strength data with mixed and cohesive failure modes becoming more prevalent in the study group as compared to the control group. In clinical terms, this indicated that the interface was no longer the weakest part of most of the study specimens, but the propagation of stresses was instead partly through the resin cement or across the more integrated interfacial zone. This is a good result as adhesive failure at zirconia is frequently linked to reduced long-term retention, and risk of marginal leakage and debonding of minimally retentive restorations. Abdou et al. also demonstrated that the performance of zirconia bond increased with surface pretreatment in conjunction with an MDP-containing primer and MDP-containing self-adhesive cement, and failure modes indicated increased integrity of the interface [31]. Reduction in adhesive failure from 68% to 16% is significant in that it is not only statistically significant but also is mechanistically consistent with the XPS/FTIR evidence presented in Figure 1. The study group seems to have been able to alter the mechanical preparation, but chemically inadequate surface of zirconia into a more wettable and more reactive surface for more uniform interactions between resin cement and zirconia. Khanlar et al. found that the bond durability to high-translucent zirconia might be improved by implementing silicatization and silanization protocols, particularly by generating a silica-containing surface modification of zirconia that is suitable for resin bonding through a silane-mediated approach. This is in line with the current observation that an interfacial chemistry that is silicatized can help decrease solely adhesive failure after aging [32]. The current pattern of failure modes also correlates with the reported reduction in hydrolytic degradation and higher likelihood of non-adhesive failure following thermocycling when MDP-based primers are used. In highly translucent zirconia, the bond strength and hydrolytic aging of the bonded interface were improved after application of the MDP-based primer in addition to airborne-particle abrasion, Xiong and co-authors reported. The present research is an extension of the above idea in which it is proposed that plasma activation and a silicatized calcium-phosphate nanolayer can be used as a chemically enriched platform on which phosphate- and silane-compatible reactions can be made more durable [33].

An important clinical explanation for the strong bonding without aggressive surface damage obtained in the study group is given in Table 4. For the control group, the Ra and Rq were significantly higher, which fits with the craters, grooves and embedded alumina residues produced from airborne-particle abrasion. The study group exhibited significantly less roughness and much less contact angle, suggesting that the mechanisms were not just roughness, but also wettability and surface chemistry. On the contrary, Falahchai et al. observed that airborne-particle abrasion enhanced the roughness and resulted in high shear bond strength for all types of zirconia with varying yttria content, with mechanical retention being a good bonding approach [34]. The reduced roughness in the study group could be clinically beneficial for translucent 5Y zirconia, as surface defects might affect flexural strength and optical characteristics. Alumina and glass-bead blasting were shown to improve zirconia bonding, when combined with chemical treatment, as reported by Abdou and colleagues, but also resulted in rougher surfaces and lower contact angles than untreated controls. The present study is a compromise as it achieved significantly better wettability than the control with a smoother surface that may account for the benefit seen in bond strength, reliability, optical behavior, and flexural strength [31]. This interpretation is supported by the SEM alteration score in Table 4, which indicates that the control surface was severely altered, while the study surface was only mildly altered. This means that the plasma–silicatized calcium-phosphate protocol might be better for thin veneers, anterior crowns, and minimally retentive restorations made of high-translucency zirconia in which deep surface flaws are not desired. Kim and colleagues showed that sandblasting also causes subsurface phase and stress changes in 3Y-, 4Y- and 5Y-zirconia, and that the level of damage varied according to the particle size, which is another reason why the surface modification route used in the present study was preferred to be less destructive [35].

The chemical evidence to explain the mechanical and failure-mode results is given in Figure 1. The study group demonstrated positive standardized differences with respect to oxygen signal, silicate enrichment, calcium enrichment, phosphate enrichment, hydroxyl-rich O 1s component, FTIR Si–O–Si band intensity, FTIR PO4 band intensity, and O/C ratio while carbon contamination and alumina residue were less. This combination is evidence of surface cleaning, inorganic functionalization and chemically active nanolayer formation. Using

XRD, ATR-FTIR, XPS, and SEM, Shen and co-authors also demonstrated that the glass-ceramic spray deposition could create silicate-related surface chemistry on zirconia and enhance the bond strength of zirconia after thermal cycling when compared to conventional methods [36]. This is clinically important because the lower contamination by carbon in Figure 1 can reduce the masking of the reactive zirconia hydroxyl groups and increase the interaction between the primer and the group. Plasma treatment is known to increase surface energy by causing removal of organic contaminants and creation of polar oxygen-containing groups, and these are reflected in the increase in O/C ratio and decrease in contact angle in the present study. Recently, Wu et al. demonstrated that the physicochemical properties of zirconia surfaces could be altered when the glass-ceramic spray deposition was accompanied by handheld nonthermal plasma augmentation, thus indicating that plasma could be used not only as a topographic modification tool, but also as a chemical activator [37]. A second biologically and chemically meaningful dimension was provided by the calcium and phosphate enrichment in Figure 1. Zirconia is chemically inactive, but polar ionic sites and hydroxyl-rich chemistry can be added by zirconia functionalization with calcium-phosphate to enhance wettability and resin-cement adaptation. Cheng and associates said alkaline treatment and calcium-phosphate coating modified the surface properties of zirconia for implant-related applications, which lent credence to the concept that calcium-phosphate modification could transcend zirconia's inertness. The present study extends this idea to adhesive dentistry, where the ultimate clinical objective is not osseointegration but enhancement of the durability of the cement–ceramic interface [38]. The high intensity of the FTIR signals of the silicate and phosphate also contributed to understanding lower adhesive failures in the study group. Surface chemistry that involves silicates can assist the silane-compatible bond and phosphate-related surface chemistry can complement MDP-type phosphate-monomer interactions. Yoshida found that the bond between the resin cement and zirconia increased as the concentration of MDP was raised in the primers up to an optimum level, and that the MDP-containing primer groups resulted in greater bond strength than the controls after thermal cycling. This is in line with the present findings that phosphate-compatible chemistry is clinically applicable, but the present protocol differs in that it involves the generation of a reactive phosphate-containing surface chemistry, and not just the concentration of the primer [39]. The reduced alumina residue in Figure 1 is also desirable since inclusions of alumina might lead to micromechanical roughness but do not ensure a chemically optimum bonding surface. Khanlar et al. showed that bond strength and surface topography of the high-translucent zirconia was affected by air-particle abrasion treatments and that clinical benefit was related to treatment parameters and the use of a primer. The present study indicates that it is possible to reduce the alumina contamination and increase the silicate, calcium, phosphate and hydroxyl signals and thus change the bonding mechanism from defect-driven retention to chemical surface integration [32].

As illustrated in Figure 2, the plasma–silicatized calcium-phosphate treatment/aging protocol resulted in better post-treatment/aged translucency, less translucency loss, a lower color difference, and a higher biaxial flexural strength, although it did not significantly increase the monoclinic phase fraction. Clinically, this is another excellent combination for 5Y zirconia, as the esthetic zirconia needs to be optically stable yet sturdily strong after surface treatment. McLaren et al. discovered that the strength of translucent zirconia was determined by the yttria content and treatment of the surface: particularly, alumina airborne-particle abrasion produced the roughest surface and had a deleterious effect on strength for the 5Y materials. This corroborates the results of the present study, where a smoother chemically activated treatment was able to maintain or enhance the mechanical behavior of 5Y zirconia [40].

The clinically important monoclinic phase difference shown in Figure 2 is nonsignificant, since this means that the experimental treatment did not compromise the aging of 5Y zirconia. The presence of a high fraction of cubic-phase makes the 5Y zirconia a low transformation potential material, so a higher monoclinic content after surface treatment would not reflect a beneficial transformation toughening, but more likely a detrimental phase destabilization. Kim et al. reported that such phase transformations and subsurface stresses can be created by sandblasting, depending on the grade of the zirconia and the size of the alumina particles, so the current finding that the study protocol was successful in creating surface activation without clinically relevant phase damage is supported [32]. The optical results shown in Figure 2 are especially significant for anterior and esthetic-zone restorations. The translucency of the baseline was not significantly different which confirmed initial comparability; however, the translucency of the study group was higher and the ΔTP and ΔE00 were lower after treatment and aging. This resulted in the experimental protocol being less optically disruptive than the control, and it may lessen the potential for shade mismatch or opacity increase post-cementation. Cho et al. demonstrated that translucency and masking ability of dental zirconia are greatly affected by yttria content which proved to be a material-sensitive outcome and should be preserved during any surface treatment [41]. The lower color difference in the study group may be due to lower roughness and less severe SEM alteration presented in Table 4. Rough surfaces produce more scattering, have residue retention, and can alter the value and chroma of high-translucency ceramics. Hemmati and coworkers showed that after thermocycling with coffee, the color stability and translucency of full cubic stabilized zirconia were influenced by surface treatment and bonding procedures; that is, the surface modification could have visible esthetic effects. In the present study, the lower ΔE00 is thus in favor of the clinical safety of plasma–silicatized protocol for esthetic zirconia restorations [42]. This is clinically significant as the higher biaxial flexural strength of the study group is a significant advantage with surface treatment methods that are known to increase bonding, which typically lower the strength of the ceramic material due to the presence of microcracks. The present study indicates that chemical activation and nanolayer formation may be beneficial at increasing bonding without introducing the flaw population characteristic of aggressive abrasion. The present interpretation is that surface treatments and cyclic fatigue may affect subsurface defects and mechanical properties of zirconia frameworks as reported by Elraggal and colleagues and thus should be tested in conjunction with bond strength [43]. The present results further compare favorably with the studies demonstrating the compromise between translucency and mechanical strength in the case of high-yttria zirconia. Jerman et al. indicated differences between 3Y-, 4Y- and 5Y-zirconia in translucency, hardness, biaxial flexural strength, and fracture toughness, noting that the more translucent zirconias typically demand more conservative surface conditioning. In that frame, the setting of the current study, which offers higher aged bond strength, better optical preservation and higher flexural strength, is clinically significant as it focuses on the main problem of 5Y zirconia, which is the need for adhesive reliability without sacrificing strength or esthetics [44].

The present study is partly justified by reliability studies that indicated various types of aging behavior between the different grades of zirconia and that the strength retention is related to the microstructure and surface condition. Spies and collaborators found that the different zirconia grades that were used for monolithic fixed dental prostheses presented

different reliability and aging behavior, supporting the simultaneous assessment of aged bond strength, Weibull reliability, optical change, and flexural strength. The integrated result pattern of the present study is thus more significant than a bond-strength-only conclusion because it indicates that adhesion was not obtained at the expense of material reliability for the experimental surface [45]. The results here do not completely agree with the studies that showed that airborne-particle abrasion was the best conditioning method. However, as reported by Zhao et al., the bond strength of highly translucent zirconia is influenced by the parameters of the airborne-particle abrasion process, so that abrasion pressure and particle conditions should not only be avoided but also be optimized. The current study does not contradict that evidence but does indicate that the plasma–silicatized calcium-phosphate treatment may be an alternative if simultaneous bonding, esthetics, and the maintenance of 5Y zirconia strength are the primary clinical considerations [46]. The results are also in line with studies where silica-related surface treatments have demonstrated to be comparable or superior to alumina abrasion for the correct surface chemistry. Thammajaruk et al. demonstrated that lithium-disilicate glass-coated zirconia achieved clinically relevant resin-cement bonding when compared with alumina air-abraded zirconia. This corroborates the existing XPS/FTIR interpretation that the formation of silicate is not only a surface indicator but also a functional adhesive feature especially in conjunction with plasma cleaning and a calcium-phosphate component [47]. The present research also supports the findings that the choice of surface-treatment needs to take into account the yttria content of zirconia. The effect of yttria content on the microstructure, phase stability and mechanical properties of dental zirconia is reported by Li et al., which explains why a protocol that is safe for 3Y-TZP may not be optimal for 5Y zirconia. The study protocol seems to be appropriate for 5Y zirconia because of the lowest amount of monoclinic transformation, maintenance of translucency, decreased color change and enhanced strength after aging [48]. These results also argue for the general idea of surface activation, optimized without excessive roughness. Based on the results of Sales and colleagues, the various surface treatments of zirconia did have a significant impact on micro-shear bond strength and surface characteristics, indicating that bond performance is also chemistry dependent and topography dependent. The present study extends that by showing that even a low-Ra, low-Rq surface can yield excellent aged adhesion, if wettability and inorganic surface chemistry are well enhanced, and question the previously held view that roughness is the primary factor in zirconia bonding [48]. The current study confirmed, from a clinical point of view, the applicability of plasma–silicatized calcium-phosphate nanolayer formation as a conservative conditioning procedure for high-translucency zirconia restorations, particularly in situations where esthetics, thin ceramic geometry and long-term retention are all important. All the results together—increased aged bond strength, improved Weibull behavior, reduced adhesive failures, improved wettability, reduced roughness, reduced optical degradation, unchanged phase stability and increased flexural strength—constitute a compelling case that the protocol leads to better interface quality without compromising the strength of the ceramic. Recent orthodontic and restorative zirconia studies also stress that there is a need to balance mechanical and chemical surface treatments and not just choose the strongest bond [49].

Conclusion

Atmospheric plasma activation combined with deposition of an ultrathin silicatized calcium-phosphate nanolayer achieved a more effective and conservative bonding strategy for hydrothermally aged 5Y translucent zirconia than did conventional airborne-particle abrasion combined with an MDP-containing primer. The experimental protocol resulted in significant increases in aged resin–zirconia bond strength and better bond reliability, as evidenced by the higher mean bond-strength values, higher Weibull modulus, and higher characteristic strength. The shift from predominantly adhesive failure in the conventional group toward mixed and cohesive resin-cement failure in the study group was also shown, which further confirmed the mechanical and chemical stability of the modified interface in the study group as compared to the conventional group. The good bonding capability was believed to have come from a better surface activation and functionalization, rather than from the use of an aggressive mechanical roughening. The plasma–silicatized calcium-phosphate nanolayer protocol created an extremely wettable surface with considerably lower water contact angle and much lower roughness and less destructive surface alteration than the airborne-particle abrasion protocol. XPS and ATR-FTIR results indicated an enrichment of silicate, calcium, phosphate and hydroxyl-related components, which helped to achieve a successful formation of a chemically active nanolayer that enhances the interaction with the MDP-containing primer and resin cement. Importantly, this improved interfacial performance was not accompanied by clinically problematic phase destabilization, as monoclinic transformation was low in both groups. Additionally, the study treatment exhibited better optical preservation, less color change, less loss of translucency, and higher flexural strength, indicating that the ultrathin nanolayer method may be ideal for highly translucent zirconia restorations that demand optical translucency and structural integrity. Long-term laboratory and clinical studies are needed to confirm the durability, reproducibility and clinical application of this minimally invasive plasma-assisted nanolayer bonding protocol. appropriately and to standardize them whenever possible.

Conflicts of interest

The authors declare no competing interest.

References

1. Fernando, Z., Russo, S., & Sorrentino, R. (2011). From porcelain-fused-to-metal to zirconia: Clinical and experimentalconsiderations. Dental Materials, 27, 83–96. https://doi.org/10.1016/j.dental.2010.10.024
2. Blatz, M. B., Phark, J.-H., Ozer, F., Mante, F. K., Saleh, N., Bergler, M., & Sadan, A. (2010). In vitro comparative bond strength of contemporary self-adhesive resin cements to zirconium oxide ceramic with and without air-particle abrasion. Clinical Oral Investigations, 14, 187–192. https://doi.org/10.1007/s00784-009-0278-0
3. Burke, F. J., Fleming, G. J., Nathanson, D., & Marquis, P. M. (2002). Are adhesive technologies needed to support ceramics? An assessment of the current evidence. Journal of Adhesive Dentistry, 4, 7–22.
4. Huang, B., Chen, M., Wang, J., & Zhang, X. (2024). Advances in zirconia-based dental materials: Properties, classification, applications, and future prospects. Journal of Dentistry, 147, 105111. https://doi.org/10.1016/j.jdent.2024.105111
5. Shahmiri, R., Standard, O. C., Hart, J. N., & Sorrell, C. C.(2018).Optical properties of zirconia ceramics for estheticdentalrestorations: A systematic review. Journal of Prosthetic Dentistry,119,36–46. https://doi.org/10.1016/j.prosdent.2017.07.009
6. Khan, A. A., Al Kheraif, A. A. A.,Jamaluddin,S.,Elsharawy, M., & Divakar, D. D. (2017). Recent trends in surface treatment methods for bonding composite cement to zirconia: A review. Journal of Adhesive Dentistry,19,7–19. https://doi.org/10.3290/j.jad.a37720

7. Inokoshi, M., De Munck, J., Minakuchi,S.,&VanMeerbeek,B. (2014). Meta-analysis of bonding effectiveness to zirconia ceramics. Journal of Dental Research,93, 329–334. https://doi.org/10.1177/0022034514524228
8. Komine, F., Markus, B. B., &Hideo, M. (2010). Current status of zirconia-based fixed restorations. Journal of Oral Science,52,531–539. https://doi.org/10.2334/josnusd.52.531
9. Lung,C. Y. K., & Matinlinna, J. P. (2012). Aspects of silane coupling agents and surface conditioning in dentistry:An overview. DentalMaterials,28,467–477. https://doi.org/10.1016/j.dental.2012.02.009
10. Alrabeah, G., Alomar, S., Almutairi, A., Alali, H., & ArRejaie,A. (2023). Analysis of the effect of thermocycling on bonding cements to zirconia. Saudi Dental Journal,35,734–740. https://doi.org/10.1016/j.sdentj.2023.07.009
11. D'Amario,M., Campidoglio, M., Morresi, A. L., Luciani, L., Marchetti, E., & Baldi, M.(2010).Effect of thermocycling on the bond strength between dual-cured resin cements and zirconium-oxide ceramics. Journal of Oral Science, 52, 425–430. https://doi.org/10.2334/josnusd.52.425
12. Rigos, A. E., Sarafdou, K., & Kontonashi, E. (2023). Zirconia bond strength durability following artificial aging: A systematic review and meta-analysis of in vitro studies. Japanese Dental Science Review,59,138–159. https://doi.org/10.1016/j.jdsr.2023.04.002
13. Sladek, R. E. J., & Stoffels, E. (2005). Deactivation of Escherichia coli by the plasma needle. Journal of Physics D: Applied Physics, 38,1716. https://doi.org/10.1088/0022-3727/38/11/012
14. Sladek, R. E. J., Stoffels, E., Walraven, R., Tielbeek, P. J. A., & Koollhoven, R. A. (2004). Plasma treatment of dental cavities: A feasibility study. IEEE Transactions on Plasma Science, 32, 1540–1543. https://doi.org/10.1109/TPS.2004.832636
15. Laroussi, M., Tendero, C., Lu, X., Alla, S., & Hynes, W. L. (2006). Inactivation of bacteria by the plasma pencil. Plasma Processes and Polymers, 3, 470–473. https://doi.org/10.1002/ppap.200600005
16. Cha, S., & Park, Y. S. (2014). Plasma in dentistry. Clinical Plasma Medicine, 2, 4–10. https://doi.org/10.1016/j.cpme.2014.04.002
17. Silva, N. R., Coelho, P. G., Valverde, G. B., Becker, K., Ihrk, R., Quade, A., & Thompson, V. P. (2011). Surface characterization of Ti and Y-TZP following non-thermal plasma exposure. Journal of Biomedical Materials Research Part B: Applied Biomaterials,99, 199–206. https://doi.org/10.1002/jbm.b.31887
18. Aanaszak, A., Terefinko, D., Motyka-Pomagruk,A., Grzebieluch, W., Wdowiak, J.,Pohl,P.,Śledź,W.,Malicka, B., Jamroz, P., Skoskiewicz-Malinowska,K.,etal. (2025). Possibilities of application of cold atmospheric pressure plasmas in dentistry—A narrative review. Plasma Processes and Polymers,22, e2400246. https://doi.org/10.1002/ppap.202400246
19. Ritts, A. C., Li, H., Yu, Q., Xu, C., Yao, X., Hong, L., & Wang, Y. (2010). Dentin surface treatment using a non-thermal argon plasma brush for interfacial bonding improvement in composite restoration. European Journal of Oral Sciences, 118, 510–516. https://doi.org/10.1111/j.1600-0722.2010.00761.x
20. Liu, Y., Liu, Q., Yu, Q. S., & Wang,Y.(2016a).Nonthermal atmospheric plasmas in dental restoration. Journal of Dental Research, 95, 496–505. https://doi.org/10.1177/0022034516629425
21. Ito, Y., Okawa, T., Fujii, T., & Tanaka, M. (2016). Influence of plasma treatment on surface properties of zirconia. Journal of Osaka Dental University, 50, 79–84.
22. Liu, T., Hong, L., Hottel, T., Dong, X., Yu, Q., & Chen, M. (2016b). Non-thermal plasma enhanced bonding of resin cement to zirconia ceramic. Clinical Plasma Medicine, 4, 50–55. https://doi.org/10.1016/j.cpme.2016.08.002
23. Ye, X. Y., Liu, M. Y., Li, J., Liu, X. Q., Liao, Y., Zhan, L. L., Zhu, X. M., Li, H. P., & Tan, J. (2022). Effects of cold atmospheric plasma treatment on resin bonding to high-translucency zirconia ceramics. Dental Materials Journal, 41, 896–904. https://doi.org/10.4012/dmj.2022-068
24. Miura, S., Fujisawa, M., Vallittu, P., & Lassila, L. (2024). Effects of plasma surface treatment on the bond strength of zirconia with an adhesive resin luting agent. Dental Materials Journal,43,582–590. https://doi.org/10.4012/dmj.2024-051
25. Alshali, R. Z., Alqahtani, M. A., Alturki, B. N., Algizani, L. I.,Batarfi,A. O., Alshamrani, Z. K.,Faden, R. M., Bukhary, D. M., & Altassan, M. M. (2024). Effect of air-particle abrasion and methacryloyloxydecyl phosphate primer on fracture load of thin zirconia crowns: An in vitro study. Frontiers in Dental Medicine, 5, 1501909. https://doi.org/10.3389/fdmed.2024.1501909
26. Khanlar, L. N., Takagaki, T., Abdou, A., Kusumasari, C., Rezvani, A. J., Rizk, A. M., Hosaka, A. E., & Tagami, J. (2022). Effect of air-particle abrasion protocol and primer on the topography and bond strength of a high-translucent zirconia ceramic. Journal of Prosthodontics,31(3),228–238. https://doi.org/10.1111/jopr.13372
27. Liao, Y., Phan, T., & Yu, Q. (2025). Cold atmospheric plasma treatment of zirconia to improve its bond strength and longevity with dental cement.Materials,18(15), 3482. https://doi.org/10.3390/ma18153482
28. Alammar, A., & Blatz, M. B. (2022). The resin bond to high-translucent zirconia—A systematic review. Journal of Esthetic and Restorative Dentistry, 34(1), 117–135. https://doi.org/10.1111/jerd.12876
29. Samran A. Ali S, El Bahra S, Hashem AW, Elbeshiri M, Willie S, Kern M. (2025). Durability of resin bonding to transluscent zirconia materials: An in vitro study. J Prosthet Dent, 133(6), 1583.e1-1583.e8. https://doi.org/10.1016/j.prosdent.2025.03.017
30. Alnazzawi AA, AbdElaziz MH, Farghal AE, Aldamaty MF, Borzangy S, Ainoosah S, Alqutaibi AY. (2025). Effect of different surface treatments on the bond strength of different monolithic zirconia with dentin. Int Dent J, 75(4), 100812. htpps://doi.org/10,.1016/j.ident.2025.03.021
31. Abdou, A., Hussein, N., Abd El-Sattar, N. E. A., Takagaki, T., Kusumasari, C., Rizk, A., & Abo-Alazm, E. A. (2023). MDP-salts as an adhesion promoter with MDP-primers and self-adhesive resin cement for zirconia cementation. BMC Oral Health, 23, 874. https://doi.org/10.1186/s12903-023-03663-y
32. Khanlar, L. N., Takagaki, T., Abdou, A., Inokoshi, M., Ikeda, M., Nikaido, T., & Tagami, J. (2022). The effects of different silicatization and silanization protocols on the bond durability of resin cements to new high-translucent zirconia. Clinical Oral Investigations, 26, 3547–3561. https://doi.org/10.1007/s00784-021-04323-7
33. Xiong Y, Zhao P, Jin C, Wang J, Arola D, Gao S. Effect of airborne-particle abrasion protocols and MDP-based primer on the bond strength of highly translucent zirconia. (2021). J Adhes Dent, 23(5), 437-446. https://doi.org/10.3290/j.jad.b2000249
34. Falahchai, M., Neshandar Asli, H., Faghani, M., & Hendi, A. (2024). Effect of different surface treatments on shear bond strength of zirconia with various yttria contents. BMC Oral Health, 24, 1520. https://doi.org/10.1186/s12903-024-05348-6
35. Kim HK, Yoo KW, Kim SJ, Jung CH. (2021). Phase transformations and subsurface changes in three dental zirconia grades after sandblasting with various Al(2)O(3) particle sizes. Materials (Basel), 14(18), 5321. https://doi.org/10.3390/ma14185321

36. Shen, D., Wang, H., Shi, Y., Su, Z., Hannig, M., & Fu, B. (2023). The effect of surface treatments on zirconia bond strength and durability. Journal of Functional Biomaterials, 14(2),89. https://doi.org/10.3390/jfb14020089

37. Wu SH, Lai SY, Lee IT, Mine Y, Huang HY, Peng TY. Handheld nonthermal plasma augmentation of glass-ceramic spray deposition on zirconia surface characterization and MG-63/HGF-1 cell behavior: an in vitro study. (2025). J Funct Biomater, 16(11), 421. https://doi.org/10.3390/jfb16110421

38. Cheng, M.-S., Chen, C.-Y., Hsu, S.-M., & Chang, Y.-Y. (2022). Preparation of calcium phosphate compounds on zirconia ceramics by alkaline treatment and coating procedures.Materials, 15(12),4227. https://doi.org/10.3390/ma15124227

39. Yoshida, K. (2021). Effect of 10-methacryloyloxydecyl dihydrogen phosphate concentrations in primers on bonding resin cements to zirconia. Journal of Prosthodontics,30(4),356–362. https://doi.org/10.1111/jopr.13255

40. McLaren, E. A., Maharishi, A., & White, S. N. (2023). Influence of yttria content and surface treatment on the strength of translucent zirconia materials. The Journal of Prosthetic Dentistry, 129(4), 638–643. https://doi.org/10.1016/j.prosdent.2021.07.001

41. Cho, Y.-E., Lim, Y.-J., Han, J.-S., Yeo, I.-S. L., & Yoon, H.-I. (2020). Effect of yttria content on the translucency and masking ability of yttria-stabilized tetragonal zirconia polycrystal. Materials, 13(21), 4726. https://doi.org/10.3390/ma13214726

42. Hemmati YB, Asli HN, Nahavandi AM, Safari N, Falanchai M. (2023). Effect of orthodontic bonding with different surface treatments on color stability and translucency of full cubic stabilized zirconia after coffee thermocycling. Korean J Orthod, 53(3), 139-149. https://doi.org/10.4041/kjod22.144

43. Elraggal A, Silikas N. (2021). Effect of air-abraded versus laser-fused fluorapatite glass-ceramics on shear bond strength of repair materials to zirconia. Materials (Basel), 14(6), 1468. https://doi.org/10.3390/ma14061468

44. Jerman E, Lümkemann N, Eichberger M, Hampe R, Stawarczyk B. (2021). Impact of varying step-stree protocols on the fatigue behavior of 3Y-TZP, 4Y-TZP and 5Y-TZP ceramic. Dent Mater, 37(7), 1073-1082. https://doi.org/10.1016/j.dental.2021.03.013

45. Spies, B. C., Zhang, F., Wesemann, C., Li, M., & Rosentritt, M. (2020). Reliability and aging behavior of three different zirconia grades used for monolithic four-unit fixed dental prostheses. Dental Materials,36(10),e329–e339. https://doi.org/10.1016/j.dental.2020.08.002

46. Zhao, P., Yu, P., Xiong, Y., Yue, L., Arola, D., & Gao, S. (2020). Does the bond strength of highly translucent zirconia show a different dependence on the airborne-particle abrasion parameters in comparison to conventional zirconia? Journal of Prosthodontic Research, 64(1), 60–70. https://doi.org/10.1016/j.jpor.2019.04.008

47. Thammajaruk,P.,Buranadham, S., Guazzato, M., & Wang, Y. (2021). Shear bond strength of composite cement to lithium-disilicate glass-coated zirconia versus alumina-air-abraded zirconia.The Journal of Adhesive Dentistry, 23(3), 267–275. https://doi.org/10.3290/j.jad.b1367913

48. Li, Q.-L., Jiang, Y.-Y., Wei, Y.-R., Swain, M. V., Yao, M.-F., Li, D.-S., & Zhang, F. (2022). The influence of yttria content on the microstructure, phase stability and mechanical properties of dental zirconia. Ceramics International, 48(4), 5361–5368. https://doi.org/10.1016/j.ceramint.2021.11.079

49. Sales, A., Rodrigues, S. J., Mahesh, M., Ginjupalli, K., Shetty, T., Pai, U. Y., & Kotian, R. (2022). Effect of different surface treatments on the micro-shear bond strength and surface characteristics of zirconia: An in vitro study. International Journal of Dentistry, 2022, 1546802. https://doi.org/10.1155/2022/1546802

50. Limpuangthip,N.,Surintanasarn, A., & Vitavaspan, P. (2023). Mechanical and chemical surface treatment enhances bond strength between zirconia and orthodontic brackets: An in vitro study. BDJ Open, 9, 53. https://pubmed.ncbi.nlm.nih.gov/38065947/.

Table 1. Baseline dimensions, surface roughness, wettability, translucency, and color characteristics of 5Y translucent zirconia specimens before bonding.

Parameter	Control group (n=25)	Study group (n=25)	Mean difference, Study–Control	95% CI	t	df	p-value
Length (mm)	12.014 ± 0.024	12.010 ± 0.025	-0.004	-0.018 to 0.010	0.557	48	0.58
Width (mm)	12.003 ± 0.029	12.009 ± 0.030	0.006	-0.011 to 0.023	-0.696	48	0.49
Thickness (mm)	1.505 ± 0.027	1.505 ± 0.014	0.001	-0.012 to 0.013	-0.137	48	0.892
Baseline Ra (µm)	0.050 ± 0.007	0.053 ± 0.008	0.003	-0.002 to 0.007	-1.27	48	0.21
Baseline Sa (µm)	0.068 ± 0.008	0.068 ± 0.006	0.000	-0.004 to 0.004	-0.183	48	0.856
Baseline contact angle (°)	74.40 ± 3.54	73.27 ± 3.19	-1.13	-3.05 to 0.79	1.186	48	0.242
Baseline translucency parameter	22.52 ± 0.90	22.64 ± 0.73	0.13	-0.34 to 0.59	-0.548	48	0.587
Baseline L*	72.08 ± 0.68	71.96 ± 0.71	-0.12	-0.52 to 0.27	0.635	48	0.529
Baseline a*	0.63 ± 0.19	0.62 ± 0.17	-0.02	-0.12 to 0.08	0.371	48	0.713
Baseline b*	8.39 ± 0.49	8.43 ± 0.46	0.05	-0.23 to 0.32	-0.34	48	0.736

Table 2. Aged resin–zirconia bond strength and Weibull reliability parameters after water storage, thermocycling, and hydrothermal aging.

Parameter	Control group (n=25)	Study group (n=25)	Difference, Study–Control	95% CI	Statistic	df	p-value
Aged bond strength (MPa)	18.33 ± 2.88	29.21 ± 3.23	10.87	9.13 to 12.61	t = -12.558	47.4	1.104e-16
Failure load (N)	20.73 ± 3.26	33.03 ± 3.66	12.3	—	—	—	—
Weibull modulus, m (95% CI)	7.60 (6.18–10.37)	9.81 (8.18–13.99)	—	—	—	—	—
Characteristic strength, σ0 MPa (95% CI)	19.53 (18.35–20.55)	30.64 (29.30–31.88)	—	—	—	—	—
Pre-test failure, n (%)	0 (0.0%)	0 (0.0%)	0.0%	—	—	—	1.0

Vol 14, No 2 (2026) DOI 10.5195/d3000/2026.1461

Table 3. Failure mode distribution after aged resin–zirconia bond strength testing.

Failure mode / comparison	Control group (n=25)	Study group (n=25)	Statistical test	P-value
Adhesive	17 (68%)	4 (16%)	—	—
Mixed	6 (24%)	15 (60%)	—	—
Cohesive within resin cement	2 (8%)	6 (24%)	—	—
Overall failure-mode distribution	—	—	Fisher–Freeman–Halton exact test	0.001
Adhesive vs non-adhesive failure	17 vs 8	4 vs 21	Fisher exact OR = 11.16	4.409e-04

Table 4. Surface morphology, roughness, and water contact angle after conventional and plasma–silicatized calcium-phosphate surface treatments.

Parameter	Control group (n=25)	Study group (n=25)	Mean difference, Study–Control	95% CI	Statistic	df	p-value
Post-treatment Ra (µm)	0.414 ± 0.055	0.086 ± 0.016	-0.328	-0.352 to -0.305	t = 28.689	27.9	2.939e-22
Post-treatment Rq (µm)	0.535 ± 0.068	0.109 ± 0.025	-0.425	-0.455 to -0.396	t = 29.3	30.4	7.912e-24
Post-treatment contact angle (°)	57.71 ± 4.0	17.65 ± 3.25	-40.07	-42.14 to -37.99	t = 38.851	46.1	7.312e-37
SEM surface alteration score (0–3)	3 (3–3)	1 (1–2)	—	—	U = 607.5	—	1.024e-09

Vol 14, No 2 (2026) DOI 10.5195/d3000/2026.1461

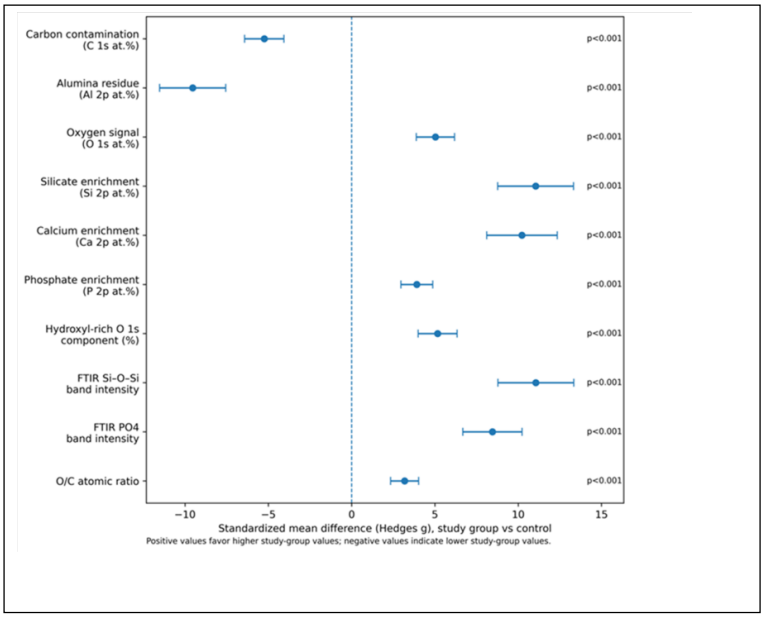

Figure 1. XPS/FTIR evidence of plasma–silicatized calcium-phosphate nanolayer formation.

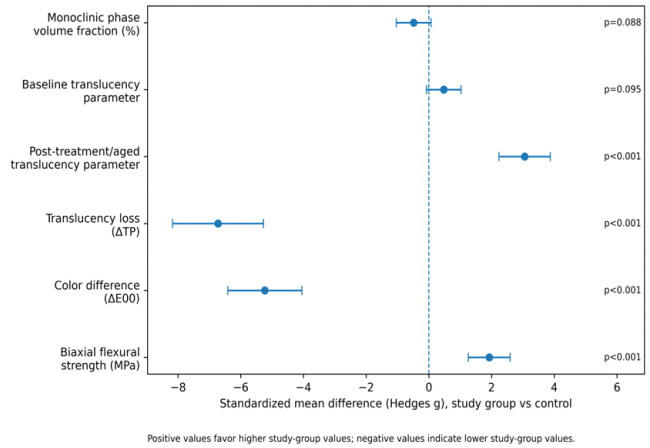

Figure 2. Phase stability, optical behavior, and flexural strength after treatment and aging.

Vol 14, No 2 (2026) DOI 10.5195/d3000/2026.1461

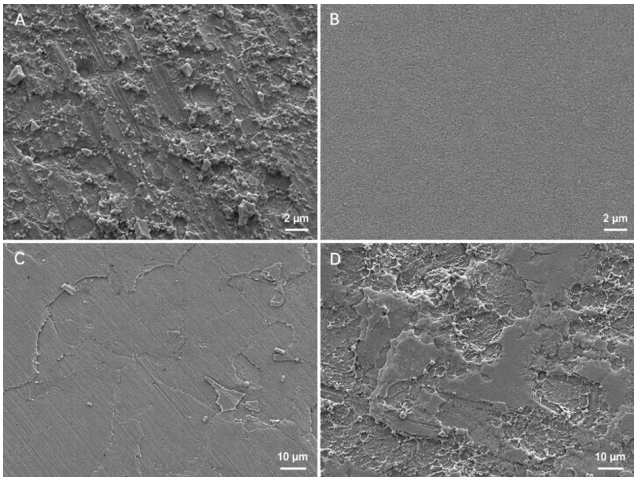

Figure 3. Scanning electron microscopic surface and fractured-interface morphology after conventional abrasion and plasma–silicatized calcium-phosphate nanolayer treatment; A: control surface, B: study surface, C: control fracture, D: study fracture.

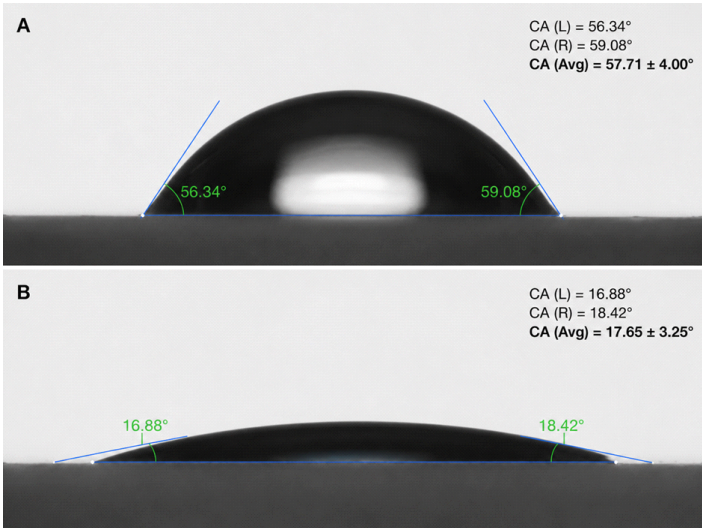

Figure 4. Direct sessile-drop contact angle images of treated 5Y zirconia surfaces; A:control group B: study group.